Progress in PHOTOVOLTAICS

PROGRESS IN PHOTOVOLTAICS: RESEARCH AND APPLICATIONS
Prog. Photovolt: Res. Appl. 2017; **25**:233–241
Published online 9 December 2016 in Wiley Online Library (wileyonlinelibrary.com). DOI: 10.1002/pip.2850

RESEARCH ARTICLE

Impact of compositional grading and overall Cu deficiency on the near-infrared response in Cu(In, Ga)Se2 solar cells

Enrico Avancini[1]*, Romain Carron[1], Benjamin Bissig[1], Patrick Reinhard[1], Roberto Menozzi[2], Giovanna Sozzi[2], Simone Di Napoli[2], Thomas Feurer[1], Shiro Nishiwaki[1], Stephan Buecheler[1] and Ayodhya N. Tiwari[1]

[1] Laboratory for Thin Films and Photovoltiacs, Empa, Swiss Federal Laboratories for Materials Science and Technology, Überlandstrasse 129, 8600 Dübendorf, Switzerland
[2] Department of Information Engineering, University of Parma, Parma, Italy

ABSTRACT

Highly efficient thin film solar cells based on co-evaporated Cu(In,Ga)Se_2 (CIGS) absorbers are typically grown with a [Ga]/([Ga] + [In]) (GGI) gradient across the thickness and a Cu-poor composition. Upon increasing the Cu content towards the CIGS stoichiometry, lower defect density is expected, which should lead to increased absorption in the near-infrared (NIR), diffusion length and carrier collection. Further, optimization of the GGI grading is expected to increase the NIR response. In this contribution [Cu]/([In] + [Ga]) (CGI) values are increased by shortening the deposition stage after the first stoichiometric point. In order to obtain comparable Ga contents at the interface for proper band alignment, the front GGI gradings were actively modified. With a relative CGI increase of 7%, we observe an increased photocurrent, originating from an improved NIR external quantum efficiency response. By characterizing the modified absorber properties by reflection-transmission spectroscopy, we attribute the observed behavior to changes in the optical properties rather than to improved carrier collection. Cu-dependent modifications of the NIR-absorption coefficients are likely to be responsible for the variations in the optical properties, which is supported by device simulations. Adequate re-adjustments of the co-evaporation process and of the alkali-fluorides post-deposition treatments allow maintaining V_{oc} and FF values, yielding an overall increase of efficiency as compared to a reference baseline. © 2016 The Authors. *Progress in Photovoltaics*: Research and Applications published by John Wiley & Sons Ltd.

KEYWORDS

Cu(In,Ga)Se2 solar cells; NIR optical response; Cu deficiency in CIGS

***Correspondence**

Enrico Avancini, Laboratory for Thin Films and Photovoltiacs, Empa, Swiss Federal Laboratories for Materials Science and Technology, Überlandstrasse 129, 8600 Dübendorf, Switzerland.

E-mail: enrico.avancini@empa.ch

Received 29 April 2016; Revised 31 August 2016; Accepted 2 November 2016

1. INTRODUCTION

Photovoltaic technologies based on polycrystalline Cu(In, Ga)Se_2 (CIGS) absorbers have gained interest thanks to their combination of high efficiency and low consumption of energy in the production process. Record values for technologies based on co-evaporated CIGS with high-temperature and low-temperature (<450 °C) processes are, respectively, 22.6% [1] and 20.4% [2] (the latest on flexible polyimide substrate). Optical losses in the near-infrared (NIR) region are among the main limitations to higher efficiencies, and are caused by incomplete absorption of NIR photons and incomplete collection of photo generated charge carriers [3]. Both loss mechanisms can lead to a decreased response in the NIR region of external quantum efficiency (EQE) spectra.

CIGS is a semiconductor with tunable direct bandgap energies depending on the indium to gallium ratio, from

1.0 eV of pure $CuInSe_2$ to 1.7 eV of pure $CuGaSe_2$ [4] mainly because of a shift in the position of the conduction band (CB) [5]. State-of-the-art absorber layers are grown by three-stage or multistage co-evaporation processes resulting in double graded material with varying [Ga]/([Ga] + [In]) (GGI) ratios across the thickness [6–9]. Typically, higher GGIs at the back and at the front and lower GGIs in the middle are targeted. The Ga-grading has three targeted functions: (i) a back surface grading resulting in a gradually decreasing CB position, which assists the drift of free electrons to the front of the absorber (back-surface field or BSF). This improves collection at NIR photon energies, as low-energy photons are absorbed far from the space-charge region [7]; (ii) a front surface grading aiming at a specific alignment of the CBs at the CdS/CIGS interface, to avoid a large potential barrier for electrons at the junction and by reaching a small favorable (<0.3 eV) [10,11] positive CB offset (CBO) between CdS and the CIGS; (iii) a low-bandgap region close to the front of the absorber for the absorption of low-energy photons. This is typically referred as the grading "notch".

Highly efficient CIGS absorbers are typically grown as a slightly Cu-poor material, with [Cu]/([In] + [Ga]) (CGI) ratios of 0.8 to 0.9 [2,12]. CIGS exhibits a large tolerance to under-stoichiometric amounts of Cu, because of the formation of stable Cu-deficient defect complexes [13–15]. Siebentritt and co-workers indicated in several publications [16–18] that higher Cu concentrations below stoichiometry can lead to improved transport properties and longer diffusion lengths. Furthermore, a recent publication [19] shows that higher Cu contents lead to steeper onsets in the absorption coefficient above bandgap energies.

In this work, we increase the final concentration of Cu and modify the grading profiles with the aim of addressing absorption in the NIR and reducing collection losses by: (i) larger notch widths, to allow larger path lengths of infrared photons in the low-bandgap region of CIGS; and (ii) higher Cu contents, to increase the NIR absorption coefficients and possibly the diffusion length. The deposition process is modified by adjusting the duration of the final deposition stage and by varying the Ga evaporation rates in order to obtain samples with different Cu content and comparable GGI ratios at the CdS/CIGS interface. Here, we report effects in the NIR region of EQE response upon a combined increase in the Cu content and in the Ga-grading notch width. Also, we report the results of electrical and material characterization of devices based on CIGS absorber layers with different Cu contents and gradings. Finally, we attempt to distinguish between the effects of optical and collection losses and to identify the mechanisms behind the observed changes in the optical properties.

2. EXPERIMENTAL

CIGS layers were grown by co-evaporation of the elements with a multi-stage low-temperature deposition process as described by Chirilă *et al.* [9] on Mo-coated (approx. 500 nm thick) soda-lime substrates. A SiO_x diffusion barrier below the Mo back contact was applied to prevent uncontrolled diffusion of alkali elements from the glass into the CIGS layer during growth. The multi-stage co-evaporation process (shown in Figure 1) consists of: a first stage in which In and Ga are evaporated; a subsequent stage in which Cu is evaporated while In and Ga rates are reduced by about one order of magnitude until a Cu-rich phase is reached; and a final stage in which again only In and Ga are deposited on the substrate to reach an overall Cu-poor composition. Additionally, In and Ga rates are varied in several sub-stages to produce the desired Ga-grading profile. Se is evaporated in overpressure throughout all stages. During the final stage, the In rate is kept constant while the Ga rate is increased to produce a front surface Ga-grading. The In source is closed shortly after the Ga source, with a final In and Se evaporation corresponding to a layer of approx. 15 nm of absorber material in which the presence of Ga and Cu because of interdiffusion is typically observed. The duration and rate of the final

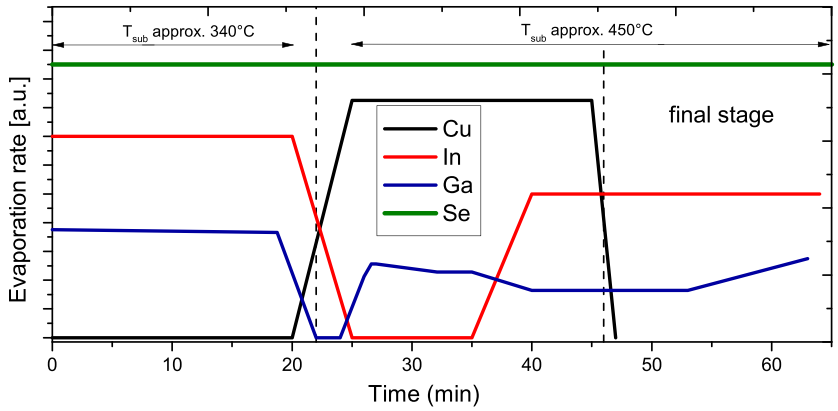

Figure 1. Schematic representation of a multi-stage deposition process with Cu, In, Ga and Se evaporation rates. The original stages of the three-stage process [20], from which the multi-stage process was adapted, are marked by the dashed vertical lines. [Colour figure can be viewed at wileyonlinelibrary.com]

2017; **25**:233–241
DOI: 10.1002/pip

Ga ramp determine the amount of Ga at the surface of the absorber, whereas the duration of the final stage determines the final concentration of Cu. In the experiments, a series of samples with different overall CGI ratios was produced by reducing the duration of the final deposition stage. For each duration of the final stage, the Ga evaporation rate during the final Ga ramp was increased so that all samples have comparable GGI ratio at the surface. Finally, sodium-fluoride (NaF) and potassium fluoride (KF) post-deposition treatments (PDTs) were applied as described in Ref.[2].

The final average CGI and GGI values of CIGS absorber layers were determined by the intensity of K-alpha lines of each element in X-ray fluorescence (XRF) measurements, calibrated with a standard absorber with a known composition.

The cells were finalized with a ca. 30 nm cadmium sulfide (CdS) buffer layer, an RF-sputtered window layer consisting of 80 nm intrinsic zinc oxide (ZnO) and 200 nm Al-doped (Al_2O_3 2 wt.%) ZnO, Ni/Al grids and a 105 nm MgF_2 anti-reflective coating.

Compositional depth profiling was measured by time-of-flight (TOF) Secondary-Ion Mass Spectrometry (SIMS), using a TOF SIMS^5 measurement unit from ION-TOF. The primary beam ions were Bi+ with 25 keV acceleration, total current of 1 pA and a raster size of $100 \times 100\,\mu m^2$. The sputtering beam was a 2 keV, 400 nA O_2+ ion source with an on-sample area of $300 \times 300\,\mu m^2$. GGI depth profiles were determined by re-scaling the total TOF-SIMS counts over their FWHM range for ^{71}Ga and ^{113}In over the average GGI composition measured by XRF.

EQE spectra were measured on completed cells with a lock-in amplifier and a chopped light source at 260 Hz followed by a triple grating monochromator at 25 °C with bias illumination with intensity close to 1000 W/m^2. The spectra were calibrated with a reference measurement of a monocrystalline Si solar cell from Fraunhofer ISE with a known response.

J–V parameters were measured using a four-terminal Keithley 2400 source meter under standard test conditions at 25 °C under 1000 W/m^2 AM1.5G illumination from an HMI sun simulator light source, which output intensity was calibrated by measuring the short-circuit current of a monocrystalline Si solar cell from Fraunhofer ISE with a known J_{sc}.

Capacitance–voltage profiles were measured with an Agilent E4980A LCR meter at a temperature of 123 K and a frequency of 300 KHz, and net free carrier concentrations were extracted at the C–V curve minimum assuming an n^+p junction following the method in References [21–24].

Transmittance–reflectance spectra were measured on batches of bare absorbers of ca. 1 cm^2 lifted from the Mo-coated substrate after gluing the surface with transparent 3 M Scotch-Weld DP100 epoxy on a transparent glass substrate dried for 2 days at room temperature and additionally for 2 h at 60 °C. The measurements were performed with a UV-3600 Shimadzu UV–VIS-NIR spectrophotometer equipped with an integrating sphere to measure total reflectance and transmittance. Spectral-dependent light absorption properties were evaluated using the function $1 - T_{abs}/(1 - R_{abs})$, where T_{abs} and R_{abs} are, respectively, spectral-dependent transmittance and reflectance measured on the lifted CIGS absorber layer. This approximation was considered to be acceptable for our purposes after comparing it with the more accurate model from Ritter and Weiser [25], which also takes into account multiple reflections at the CIGS/epoxy/glass interfaces, and finding negligible differences between the two different approximations, because of relatively weak reflection intensities at the CIGS/epoxy interface.

Additionally, the spectral-dependent reflectance R_{cell} of the completed devices was measured using the aforementioned experimental setup, together with absorptance spectra of window and buffer layers with similar composition and thicknesses as used in the solar cells. Internal quantum efficiency (IQE) spectra where then calculated as $EQE/(1 - R_{cell})(1 - A_{TCO,CdS})(1 - C_g)$ where $A_{TCO,CdS}$ is the combined absorptance from the buffer and window layer and C_g is a constant accounting for the grid coverage, in this case estimated to be 1.5% of the total area.

3. RESULTS AND DISCUSSION

The process described in Fig**ure** 1 was modified to obtain different CGI ratios by varying the duration of the final deposition stage after the first stoichiometric point. At the same time, the front Ga content was adjusted to obtain comparable front GGI ratios for all samples. The average GGI and CGI values of a set of four samples with increasing Cu contents, as measured by XRF, are shown in Table I. The GGI grading profiles are shown in Fig**ure** 2. The front end (left-hand side) of the grading profile corresponds to the interface with the CdS buffer layer, and the opposite end to the interface with the molybdenum back contact. Here, we define the Ga notch as the region with GGI values of 0.1 above the GGI minimum. The notch width w_{notch} increases by 3%, 9% and 10% as compared to the reference, respectively, for the samples with 8%, 14% and 18% CGI increase. The GGI minima decrease from 0.18 of the reference to, respectively, 0.16, 0.14 and 0.15. A double grading is present in all samples as expected from a multi-stage deposition process [26,27].

The observed changes in the Ga grading profiles in the front part of the absorber layers are a consequence of the approach chosen for varying the Cu content: as the final deposition stage is shortened, so is the duration of the final Ga ramp, bringing the notch closer to the surface [28]. Moreover, a shorter final Ga ramp leads to a reduced amount of Ga diffusion into the low-Ga notch, resulting in lower GGI minima and larger notch widths.

At the front surface of the absorber, GGI values are limited to a range between 0.28 and 0.32. The front GGI is believed to have a major influence on the performance of the completed devices as it determines the sign and size of the CBO between CIGS and the CdS buffer layer. Given the complexity of a multi-stage deposition process and the

DOI: 10.1002/pip

Table I. XRF values, *J–V* parameters and net free carrier concentration (extracted from *C–V* measurements) of the completed solar cells (average values of the three best performing cells in each six-cell sample, error values represent the standard deviation).

Sample (av. three best cells)	CGI	GGI	Voc(mV)	Jsc(mA cm^{-2})	FF(%)	η (%)	Na (cm^{-3})
Reference	0.79	0.34	719(±1)	34.7 ± 0.2	76.0 ± 0.1	19.0 ± 0.1	≤6E + 15
8% CGI increase	0.85	0.32	706(±1)	35.8 ± 0.1	75.1 ± 0.1	19.0 ± 0.1	7E + 15
14% CGI increase	0.90	0.31	701(±1)	35.2 ± 0.1	74.6 ± 0.1	18.4 ± 0.1	6E + 15
18% CGI increase	0.93	0.31	701(±1)	35.0 ± 0.1	72.9 ± 0.3	17.9 ± 0.3	3E + 15

influence of the Cu content in the diffusion of In and Ga, any attempt to vary the CGI is expected to affect the GGI grading [27–29]. The chosen approach allows obtaining Ga contents at the CIGS/CdS junction in a range which is here not assumed to severely impact the band alignment properties.

The EQE spectra of the completed solar cells are shown in Fig**ure** 3. All samples with an increased Cu content show an improvement in the NIR, i.e. an increase in the slope of the EQE curve above the bandgap. The absorption onset is determined by the chemical composition, namely the GGI and CGI (e.g. [19,30]) and by contributions from the Urbach tails. We do not further attempt to extract quantitative information from the absorption onset but compare effects at photon energies above the minimum bandgap.

Table I shows the J–V parameters of the completed solar cells as average values of the three best performing cells in each six-cell sample. The error corresponds to the standard deviation. The J_{sc} of the sample with 8% CGI increase is higher than in the reference by (1.1 ± 0.2) mA cm^{-2}, which can be attributed to the improved NIR-EQE response. Despite similar NIR-EQE behaviors, the J_{sc} is again lower for the two samples with 14% and 18% CGI increase. This is partly because of variations in the thickness of the CdS buffer layers determining the amount of parasitic absorption in the low-wavelength region (<530 nm), accounting for a difference in J_{sc} of (0.5 ± 0.1) mA cm^{-2} between the samples with 8% and 18% CGI increase. Variations in the CdS thickness are the result of temperature gradients in the CBD solution, or small differences in the amount of alkali elements evaporated on the surface during PDTs [2,31].

The NIR-EQE response is similar for all samples with an increased Cu content, despite the differences in the Cu contents and in the Ga-grading profiles among them. This could be the result of: (i) an increased collection length because of the increased Cu content [3,16], which is expected to affect the EQE mostly at long wavelengths, because NIR photons are absorbed deeper in the absorber than higher-energy photons; (ii) increased absorption length for low-energy photons because of wider low-bandgap Ga notch; and (iii) increased absorption because of larger NIR-absorption coefficients resulting from the increase in the overall Cu content as indicated by ellipsometry measurements by Minoura [19].

In the following, we discuss the abovementioned possible origins for the increased NIR response. To investigate the effect of the Cu content on the collection efficiency, parts of the bare CIGS absorber layers were removed from the Mo back and transmittance (T_{abs}) and reflectance (R_{abs}) spectra were measured on the CIGS absorbers, whereas reflectance spectra (R_{cell}) were measured on completed solar cells. The difference between the IQE and the function $1 - T_{abs}/(1 - R_{abs})$ can in a first approximation represent the spectral-dependent photocurrent collection loss. The results are shown in Fig**ure** 4.

For the samples with the 8% and 18% CGI increase, the IQE spectrum shows slightly larger values than the $1 - T_{abs}/(1 - R_{abs})$ spectra between 1000 nm and 1100 nm, which we attribute to possible minor

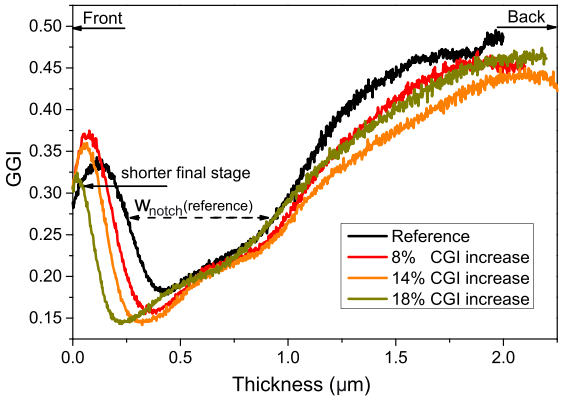

Figure 2. GGI gradings obtained by reducing the duration of the final stage and by adjusting the final Ga ramp accordingly, with increasingly higher Ga rates in the final Ga evaporation ramp. [Colour figure can be viewed at wileyonlinelibrary.com]

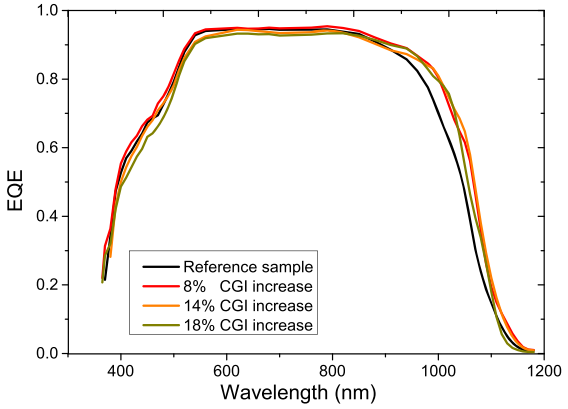

Figure 3. EQE spectra of samples with increased Cu contents and optimized front gradings. [Colour figure can be viewed at wileyonlinelibrary.com]

2017; **25**:233–241
DOI: 10.1002/pip

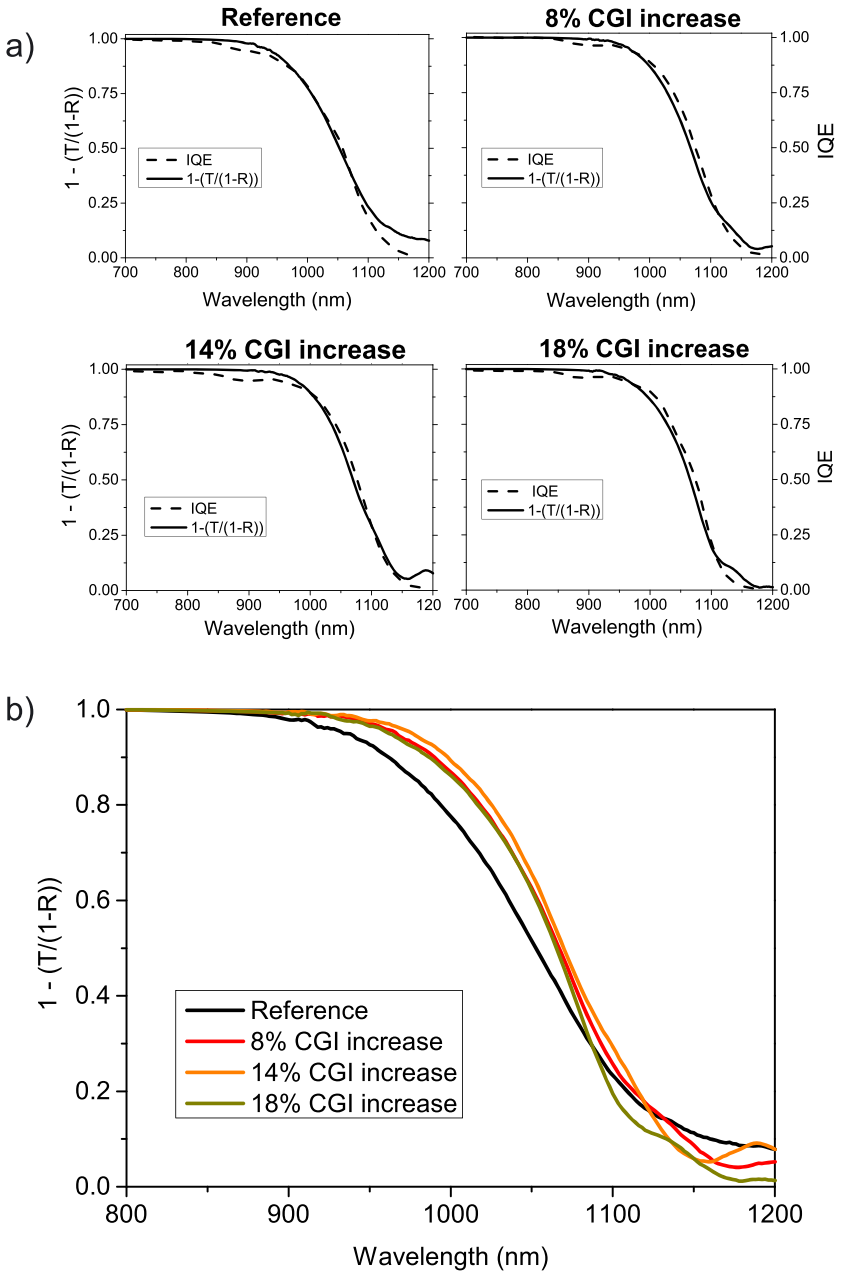

Figure 4. a) $1 - T_{abs} / (1 - R_{abs})$ and IQE spectra in the NIR-region (750 nm to 1200 nm) above the minimum bandgap for each sample listed in Table I. b) Comparison of the $1 - T_{abs} / (1 - R_{abs})$ spectra between all samples listed in Table I. [Colour figure can be viewed at wileyonlinelibrary.com]

inhomogeneities in the composition of each sample between the different areas where EQE, T_{abs} and R_{abs}, and R_{cell} were measured. Either effect is not believed to affect the conclusion of this work.

The estimated loss in photocurrent because of incomplete collection was calculated by integrating the AM1.5G spectrum with the difference between the $1 - T_{abs} / (1 - R_{abs})$ and the IQE between 800 nm and 1200 nm. For all cases, this is lower than 0.1 mA cm^{-2}. $1 - T_{abs} / (1 - R_{abs})$ spectra and IQEs show very similar behavior in the NIR, with a similar increase in the slope of the absorption onset above the optical bandgap for all the samples with increased Cu content. We exclude therefore that the observed photocurrent gain is associated to a reduction in the collection losses caused either by variations in the BSF or Cu-related changes in the material quality.

In a separate experiment (presented in Ref [32]), electron-beam induced-current (EBIC) mapping was measured on a cleaved cross section of a similar solar cell with

DOI: 10.1002/pip

a ca. 5 nm aluminum oxide passivation layer to reduce the effect of surface recombination. The results showed that the collection loss was negligible in the absorber region relevant for NIR-absorption (corresponding to the Ga notch), further confirming the observation of nearly optimal collection described above.

To investigate the role of the Ga-grading modifications, we produced two absorbers with similar Cu contents and different gradings. Both samples have a CGI of 0.9. The grading profiles and the EQE spectra are shown in Fig**ure** 5. Sample 1 has a GGI minimum at 0.21 and a notch 6% wider with respect to Sample 2 and by 13% wider with respect to the 0.79 CGI reference. Sample 2 replicates the GGI grading of the sample with 14% CGI increase in the set described earlier. EQE spectra show that Sample 2 has a smaller minimum bandgap, which correlates with the difference between the GGI minima. The slope of the EQE onset above the bandgap is slightly larger for Sample 1, which correlates with the wider notch. However, the difference in slope is much smaller than that observed between the reference and the sample with 8% CGI increase in the previous set, which had even smaller differences in notch width. Therefore, it was not possible to reproduce the changes observed in the EQEs simply by varying the GGI minimum and the notch width.

In order to further investigate the different role of the Ga grading and of the Cu content, we simulated the response of the IQE of absorbers with various gradings but same absorption function (same Cu content), and same grading but different absorption functions (different Cu content). We based these IQE simulations on the GGI gradings reported above. Absorption coefficients used in the simulations were calculated as a function of Cu and Ga contents starting from total transmittance and reflectance measurements performed on non-graded single-stage absorbers with different compositions, following a method that is explained in detail in Ref [33]. The simulations were based on the Synopsys Sentaurus-Tcad suite (as described more in detail in Ref [24,34]) and assume constant CGI across the sample and 100% collection of photocarriers.

In a first set of simulations, the gradings were kept constant, and only the Cu content was modified to investigate the effects of a variation in the Cu content on the optical properties. The grading profile chosen for this simulation corresponds to the reference sample, whereas the CGI was varied from 0.78 to 0.93, corresponding to an increase in CGI of 18%. An improvement in the IQE response, shown in Fig**ure** 6, is observed above the minimum bandgap upon increasing Cu content. This behavior is similar to the results obtained in the experiments.

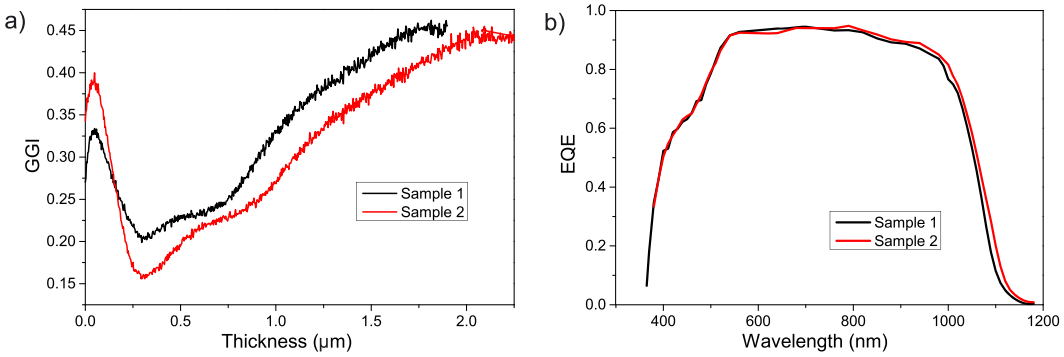

Figure 5. SIMS gradings and EQE spectra of samples with similar Cu contents (CGI increase of 14%), different Ga evaporation rates during initial and final stages of the deposition process. [Colour figure can be viewed at wileyonlinelibrary.com]

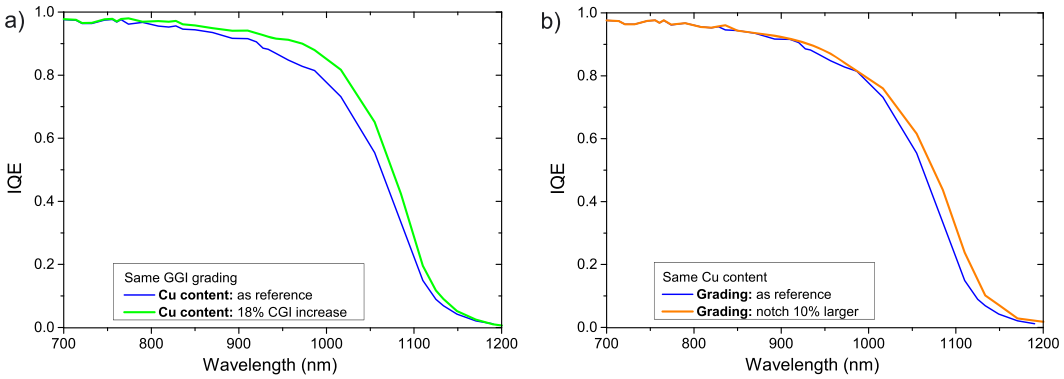

Figure 6. Simulated IQEs for (left) different Cu content, same grading and (right) different grading, same Cu content. [Colour figure can be viewed at wileyonlinelibrary.com]

2017; **25**:233–241
DOI: 10.1002/pip

Table II. Best-cell XRF values and *J–V* parameters for the reference sample and a sample with an increased Cu content and re-optimized KF-PDT and CdS CBD.

Sample (best cell)	CGI	GGI	Voc (mV)	Jsc (mA cm^{-2})	FF (%)	η (%)
Reference	0.79	0.34	718	34.7	76.1	19.0
14% CGI increase (improved interface)	0.89	0.34	718	35.9	76.8	19.9

In a second set of simulations, the Cu content was kept constant (with CGI fixed at the reference value) whereas the GGI grading was modified, according to the reference and to the sample with 18% CGI increase (10% wider notch). Besides a small shift in the position of the absorption onset, no effects on the NIR-IQE slope above the bandgap are observed. According to these simulations, the increase in the notch width alone does not explain the variations in the NIR-EQE observed in the experiments.

The increase in short-circuit current observed upon higher Cu contents, as shown in Table I, did not initially lead to any gain in efficiency as lower FFs and open-circuit voltages out-balance the J_{sc} gains. Whereas the lower open-circuit voltages could correlate with the GGI minima, the decrease in FF indicates changes in the material or interface quality. The results of C–V measurements (Table I) show, however, no trend in the net free carrier concentration N_a upon increasing Cu content.

Another experiment was performed to investigate whether the losses in open-circuit voltage and FFs could be contained despite the increase in Cu content. To re-adapt the interface properties to the modifications of the absorber composition, the overall Ga content, the KF evaporation rate during PDT and the CdS CBD deposition time were varied after a CIGS deposition process similar to the one for the sample with 14% CGI increase. Improved performance was found upon a slight increase in GGI to 0.34, a 20%–30% larger KF evaporation rate during PDT and a 20% shorter CdS–CBD. Table II shows the results for the best cell comparing the reference and the cell with increased Cu content and improved interface.

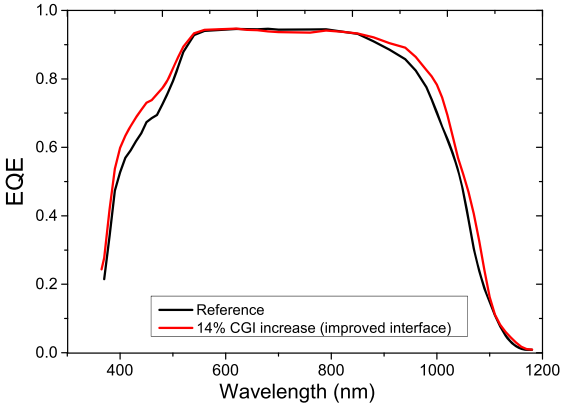

Figure 7. EQE spectra of the reference sample and the cell with 14% CGI increase and re-adjusted PDT and CBD processes. [Colour figure can be viewed at wileyonlinelibrary.com]

Along the expected increase in J_{sc}, similar values for the open-circuit voltage and a higher FF could be achieved, leading to an increase in efficiency to 19.9%. Figure 7 shows the EQE spectra of the two cells. The larger J_{sc} can be ascribed partly to a thinner CdS buffer layer and partly to the improved NIR-EQE. By integrating the EQE curves with the solar spectrum, the relative contributions to the increase in J_{sc} were calculated to be 0.5 mA cm^{-2} because of the thinner CdS and 0.7 mA cm^{-2} because of the improved NIR absorption.

Each change in the co-evaporation process for CIGS growth requires adjustments in the subsequent PDT and CBD processes, for which understanding and predictability are still lacking. The reported optimization of KF-PDT and CdS-CBD should be seen more as a technical detail rather than having scientifically relevant meaning. Nevertheless, it was possible to exploit the improved NIR absorption upon increased Cu content to obtain larger efficiencies with respect to the 0.79 CGI reference.

4. CONCLUSIONS

We produced CIGS absorbers that showed an increased response in the NIR-EQE and thus larger J_{sc} upon an increase in Cu content and wider Ga-grading notches. This was ascribed to an improved optical effect rather than to charge carrier collection effects. The improved NIR-EQE was observed after a first increase in the CGI of 8%, while further increases did not lead to further improvements. This was shown to lead to increased efficiencies with respect to a lower Cu-content reference. Re-adaptations of the surface modification treatments were necessary after the variations in the deposition process in order to obtain similar fill factors and short-circuit currents. Other experiments, confirmed by simulations, showed that an improvement in the NIR-EQE response could not be obtained by variations in the Ga grading, but mostly by exploiting different Cu-content-dependent absorption functions. It cannot be ruled out, however, that further modifications of the Ga profiles and of the absorber composition will lead to additional improvements of the NIR optical response, which could be exploited in the chase for higher efficiencies. This study shows the importance of an accurate control of the delicate balance between bandgap grading, material composition, buffer layer thickness and interface properties in determining both the optical and the electronic properties of CIGS thin films.

DOI: 10.1002/pip

ACKNOWLEDGEMENTS

This project has received funding from the European Union's Horizon 2020 Research and Innovation Programme under grant agreement No 641004 (Sharc25).

This work was supported by the Swiss State Secretariat for Education, Research and Innovation (SERI) under contract number REF-1131-52107.

This work was partially supported by the Swiss Federal Office of Energy under grant agreement SI/501145-01.

The Laboratory for Nanoscale Material Science at Empa is gratefully acknowledged for granting access to the SIMS measurement unit.

REFERENCES

1. Jackson P, Wuerz R, Hariskos D, Lotter E, Witte W, Powalla M. Effects of heavy alkali elements in Cu(In, Ga)Se2 solar cells with efficiencies up to 22.6%. *Physica status solidi (RRL)—Rapid Research Letters* 2016; **10**(8): 583–586. DOI:10.1002/pssr.201600199
2. Chirilă A, Reinhard P, Pianezzi F, Bloesch P, Uhl AR, Fella C, Kranz L, Keller D, Gretner C, Hagendorfer H, Jaeger D, Erni R, Nishiwaki S, Buecheler S, Tiwari AN. Potassium-induced surface modification of Cu(In,Ga)Se2 thin films for high-efficiency solar cells. *Nature Materials* 2013; **12**(12): 1107–11. DOI:10.1038/nmat3789
3. Siebentritt S. What limits the efficiency of chalcopyrite solar cells? *Solar Energy Materials and Solar Cells* 2011; **95**(6): 1471–1476. DOI:10.1016/j.solmat.2010.12.014
4. Scheer R, Schock HW. *Chalcogenide Photovoltaics: Physics, Technologies, and Thin Film Devices*. Whiley-VCH, Weinheim 2011.
5. Wei S, Zhang SB, Zunger A. Effects of Na on the electrical and structural properties of CuInSe2. *Journal of Applied Physics* 1999; **85**(10): 7214–7218. DOI:10.1063/1.370534
6. Contreras M, Tuttle J, Du D, Qi Y, Swartzlander A, Tennant A, Noufi R. Graded band-gap Cu(In,Ga)Se2 thin-film solar cell absorber with enhanced open-circuit voltage. *Applied Physics Letters* 1993; **63**(13): 1824–1826. DOI:10.1063/1.110675
7. Lundberg O, Bodegård M, Malmström J, Stolt L. Influence of the Cu(In,Ga)Se2 thickness and Ga grading on solar cell performance. *Progress in Photovoltaics: Research and Applications* 2003; **11**(2): 77–88. DOI:10.1002/pip.462
8. Dullweber T, Hanna G, Rau U, Schock HW. New approach to high-efficiency solar cells by band gap grading in Cu(In,Ga)Se2 chalcopyrite semiconductors. *Solar Energy Materials and Solar Cells* 2001; **67**(1-4): 145–150. DOI:10.1016/S0927-0248(00)00274-9
9. Chirilă A, Buecheler S, Pianezzi F, Bloesch P, Gretener C, Uhl AR, Fella C, Kranz L, Perrenoud J, Seyrling S, Verma RS, Romanyuk YE, Bilger G, Tiwari AN. Highly efficient Cu(In,Ga)Se2 solar cells grown on flexible polymer films. *Nature Materials* 2011; **10**(11): 857–861. DOI:10.1038/nmat3122
10. Niemegeers A, Burgelman M, Herberholz R, Rau U, Hariskos D, Schock HW. Model for electronic transport in Cu(In,Ga)Se2 solar cells. *Progress in Photovoltaics: Research and Applications* 1990**; 6(**6**)**, 407–421. http://doi.org/10.1002/
11. Klenk R. Characterisation and modelling of chalcopyrite solar cells. *Thin Solid Films* 2001; **387**(1-2): 135–140. DOI:10.1016/S0040-6090(00)01736-3
12. Jackson P, Hariskos D, Wuerz R, Wischmann W, Powalla M. Compositional investigation of potassium doped Cu(In,Ga)Se2 solar cells with efficiencies up to 20.8%. *Physica Status Solidi—Rapid Research Letters* 2014; **8**(3): 219–222. DOI:10.1002/pssr.201409040
13. Zhang SB, Wie SH, Zunger A, Katayama-Yoshida H. Defect physics of the CuInSe2 chalcopyrite semiconductor. *Physical Review B* 1998; **57**(16): 9642–9656. DOI:10.1103/PhysRevB.57.9642
14. Zhang SB, Wei SH, Zunger A. Stabilization of ternary compounds via ordered arrays of defect pairs. *Physical Review Letters* 1997; **78**(21): 4059–4062. DOI:10.1103/PhysRevLett.78.4059
15. Persson C, Zhao YJ, Lany S, Zunger A. n-Type doping of CuInSe2 and CuGaSe2. *Physical Review B—Condensed Matter and Materials Physics* 2005; **72**(3): 1–14. DOI:10.1103/PhysRevB.72.035211
16. Siebentritt S, Gütay L, Regesch D, Aida Y, Deprédurand V. Why do we make Cu(In,Ga)Se2 solar cells non-stoichiometric? *Solar Energy Materials and Solar Cells* 2013; **119**: 18–25. DOI:10.1016/j.solmat.2013.04.014
17. Deprédurand V, Tanaka D, Aida Y, Carlberg M, Fèvre N, Siebentritt S. Current loss due to recombination in Cu-rich CuInSe2 solar cells. *Journal of Applied Physics* 2014; **115**(4): 044503–8. DOI:10.1063/1.4862181
18. Aida Y, Depredurand V, Larsen JK, Arai H, Tanaka D, Kurihara M, Siebentritt S. Cu-rich CuInSe2 solar cells with a Cu-poor surface. *Progress in Photovoltaics: Research and Applications* 2014; **23**(6): 754–764. DOI:10.1002/pip.2493
19. Minoura S, Maekawa T, Kodera K, Nakane A, Niki S, Fujiwara H. Optical constants of Cu(In, Ga)Se2 for arbitrary Cu and Ga compositions. *Journal of Applied Physics* 2015; **117**(19): 195703. DOI:10.1063/1.4921300
20. Gabor AM, Tuttle JR, Albin DS, Contreras MA, Noufi R, Hermann AM. High-efficiency CuInxGa1 − xSe2

solar cells made from (Inx,Ga1 – x)2Se3 precursor films. *Applied Physics Letters* 1994; **65**(2): 198–200. DOI:10.1063/1.112670

21. Walter T, Herberholz R, Müller C, Schock HW. Determination of defect distributions from admittance measurements and application to Cu(In,Ga)Se2 based heterojunctions. *Journal of Applied Physics* 1996; **80**(8): 4411–4420. DOI:10.1063/1.363401
22. Cwil M, Igalson M, Zabierowski P, Siebentritt S. Charge and doping distributions by capacitance profiling in Cu(In,Ga)Se2 solar cells. *Journal of Applied Physics* 2008; **103**(6): 06701. DOI:10.1063/1.2884708
23. Maciaszek M, Zabierowski P, Decock K. Modeling of the impact of Se-vacancies on the electrical properties of Cu(In,Ga)Se2 films and junctions. *Thin Solid Films* 2013; **535**(1): 371–375. DOI:10.1016/j.tsf.2013.01.035
24. Sozzi G, Di Napoli S, Menozzi R, Carron R, Avancini E, Bissig B, Buecheler S, Tiwari AN, Analysis of Ga grading in CIGS absorbers with different Cu content, 43rd IEEE PVSC conference, Portland(OR) USA, June 2016.
25. Ritter D, Weiser K. Suppression of interference fringes in absorption measurements on thin films. *Optics Communications* 1986; **57**(5): 336–338. DOI:10.1016/0030-4018(86)90270-1
26. Nishiwaki S, Satoh T, Hashimoto Y, Negami T. Preparation of Cu (In, Ga) Se 2 thin films at low substrate temperatures. *Journal of Materials Research* 2001; **16**(2): 394–399
27. Reinhard P, Pianezzi F, Kranz L, Nishiwaki S, Chirilă A, Buecheler S, Tiwari AN. Flexible Cu(In,Ga)Se2 solar cells with reduced absorber thickness. *Progress in Photovoltaics: Research and Applications* 2015; **23**(3): 281–289. DOI:10.1002/pip.2420
28. Seyrling S, Chirilă A, Guettler D, Pianezzi F, Rossbach P, Tiwari AN. Modification of the three-stage evaporation process for CuIn 1 – xGaxSe2 absorber deposition. *Thin Solid Films* 2011; **519**(21): 7232–7236. DOI:10.1016/j.tsf.2010.12.146
29. Szaniawski P, Salome P, Fjallstrom V, Torndahl T, Zimmermann U, Edoff M. Influence of varying Cu content on growth and performance of Ga-graded Cu(in,Ga)Se_2 solar cells. *IEEE Journal of Photovoltaics* 2015; **5**(6): 1775–1782. DOI:10.1109/JPHOTOV.2015.2478033
30. Han SH, Hasoon FS, Pankow JW, Hermann AM, Levi DH. Effect of Cu deficiency on the optical bowing of chalcopyrite Culn 1 – xGa xSe 2. *Applied Physics Letters* 2005; **87**(15): 1–3. DOI:10.1063/1.2089154
31. Reinhard P, Bissig B, Pianezzi F, Avancini E, Hagendorfer H, Keller D, Fuchs P, Doebli M, Vigo C, Crivelli P, Nishiwaki S, Buecheler S, Tiwari AN. Features of KF and NaF postdeposition treatments of Cu(In,Ga)Se $_2$ absorbers for high efficiency thin film solar cells. *Chemistry of Materials* 2015; **27**(16): 5755–5764. DOI:10.1021/acs.chemmater.5b02335
32. Bissig B, Guerra-Nunez C, Carron R, Nishiwaki S, La Mattina F, Pianezzi F, Losio PA, Avancini E, Reinhard P, Haass S, Lingg M, Feurer T, Utke I, Buecheler S, Tiwari AN. Surface passivation for reliable measurement of bulk electronic properties of heterojunction devices. *Small* 2016; **12**(38): 5339–5346. DOI:10.1002/smll.201601575
33. Carron R, Avancini E, Bissig B, Losio PA, Ruhstaller B, Steinhauser J, Buecheler S, Tiwari AN. Oral presentation at the E-MRS Spring meeting 2016, Lille, France.
34. Sozzi G, Troni F, Menozzi M. On the combined effects of window/buffer and buffer/absorber conduction-band offsets, buffer thickness and doping on thin-film solar cell performance. *Solar Energy Materials and Solar Cells* 2014; **121**: 126–136. DOI:10.1016/j.solmat.2013.10.037

DOI: 10.1002/pip